Suppression of the gap energy in Zr-Ni-Sn and Ti-Ni-Sn by partial substitution of Zr and Ti by Ce

A. Ślebarski
Institute of Physics, University of Silesia, 40-007 Katowice, Poland

A. Jezierski
Institute of Molecular Physics, Polish Academy of Sciences, 60-179 Poznań, Poland

A. Zygmunt
Institute for Low Temperature and Structure Research, Polish Academy of Sciences, 50-950 Wrocław, Poland

S. Mähl and M. Neumann
Universität Osnabrück, Fachbereich Physik, 49069 Osnabrück, Germany

(Received 19 September 1997)

We report on magnetic measurements and electronic structure investigations of the alloyed compounds Zr-Ni-Sn and Ti-Ni-Sn. Both belong to the group of semi-Heusler alloys, and are classified as narrow-gap semiconductors with indirect gaps near 500 meV. Tetravalent ions (Zr,Ti) are partly replaced by Ce, with a Ce concentration less than 20%. Susceptibility measurements indicate the magnetic ground state of Ce in both Zr-Ni-Sn and Ti-Ni-Sn, and the effective moment is near the trivalent value at $T=300$ K. The Ce $4f^1$ configuration is well accepted by Ce $3d$ x-ray photoemission spectra. We compare the x-ray photoemission spectroscopy valence-band spectra for investigated Ce alloys. A very good agreement between the experiments and calculations is obtained. We classify Zr-Ni-Sn and Ti-Ni-Sn as alloys with a strong hybridization influence on the gap formation. The destructive alloying affecting the gap stability seems to have the same origin as in the case of Ce Kondo insulators. [S0163-1829(98)07115-X]

I. INTRODUCTION

The ternary intermetallic compounds Zr-Ni-Sn, Ti-Ni-Sn, and Hf-Ni-Sn exhibit unusual electric transport properties, suggesting that they may have a gap at the Fermi level.[1–3] These compounds crystallize in a cubic structure of the Mg-Ag-As type, and are related to the metallic Heusler alloy $M\mathrm{Ni}_2\mathrm{Sn}$, where $M=$ Zr, Ti, or Hf, and one of two sublattices is empty. The calculations of the electronic structure of several Heusler-type alloys showed semiconducting gaps for MNiSn.[4,5] In Ref. 5, Zr-Ni-Sn was classified to a group of intermetallic alloys with a strong hybridization between Zr states and conduction bands. The gap is destroyed if Ni is replaced by another transition element, e.g., by Co. The destructive influence of the substituted d element is correlated with its d occupation number. Moreover, for semi-Heusler alloys of 1:1:1 type, a gap in the electronic structure for the minority-spin direction has often been predicted by band-structure calculations, even when the transition d element replaces Ni.[5–7]

Very similar band properties are well known in the case of CeNiSn, with a small energy gap in the band structure. The ground state of CeNiSn is nonmagnetic, and low-lying excitations exhibit properties of strong correlation, analogous to those found in the heavy-fermion compound. The compounds in this class, CeNiSn,[8,9] $\mathrm{CeBi}_4\mathrm{Pt}_3$,[10] and Ce-Rh-Sb (Ref. 11) alloys, contain f elements which have unstable f configurations. The gap in CeNiSn is unstable against any change in $4f$ conduction-electron hybridization caused by alloying.[12] The gap is closed by a replacement of about 10% of either the Ni or Ce sublattice.

The electronic structures of Zr-Ni-Sn and CeNiSn are rather simple and similar. In both cases a strong hybridization effect forms the gap, and it is unstable against alloying. These arguments allow us to classify Zr-Ni-Sn or Ti-Ni-Sn and CeNiSn as intermetallic alloys with a hybridization gap at the Fermi energy.

We now present the investigation of Zr-Ni-Sn and Ti-Ni-Sn with Ce, which replaces the tetravalent M element. Ce ions under sufficiently large external or lattice pressure have a tendency to go into a mixed valence state between 3 and 4. Early experiments have indicated $4f$ instabilities for Ce in ZrIr_2, e.g., Ślebarski and Wohlleben[13,14] found Kondo-like anomalies in the resistivity and susceptibility. In Zr-Ni-Sn with tetravalent Zr, the unit-cell volume is smaller than in the corresponding mixed-valence Ce-Ni-Sn compound. Therefore, Ce impurities are expected to be under a relatively high lattice pressure. As we shall show, neither magnetic nor XPS studies have shown any instability of the $4f$ shell of Ce alloyed with Zr or Ti semi-Heusler compounds. So we expect a destructive influence of trivalent Ce with a stable $4f$ configuration on the gap in both matrices. The band calculations for several compounds, which we compared on two plots, clearly indicated that the gap directly depends on the valence of metal M in strongly hybridized materials. To our knowledge, the stability of the gap of MNiSn-type semi-Heusler alloys has not been studied experimentally up to now. We present magnetic measurements and high-resolution x-ray photoemission spectra which are in good correlation with the theory. First, we explain the gap

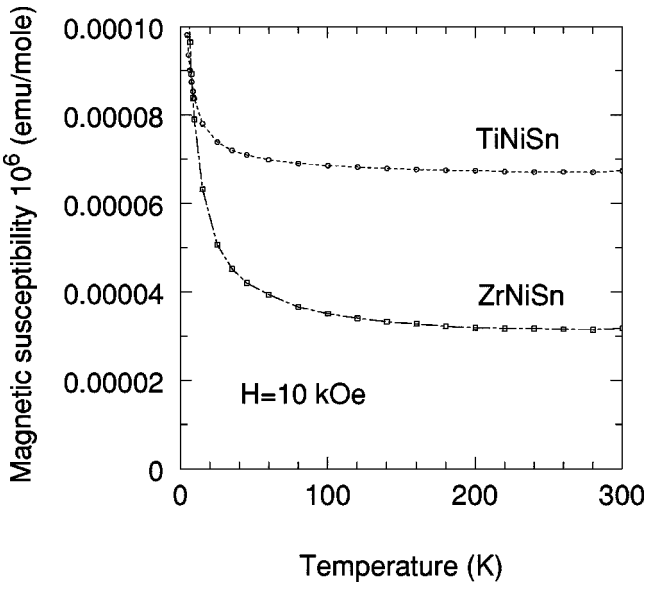

FIG. 1. Magnetic susceptibility of Zr-Ni-Sn and Ti-Ni-Sn.

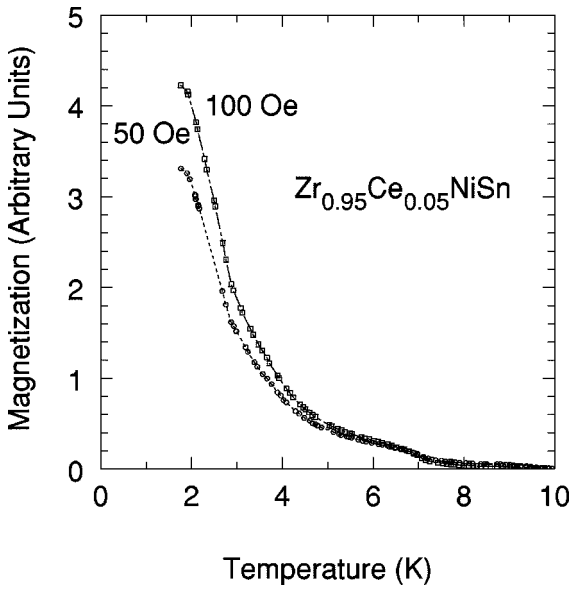

FIG. 2. Magnetization of $Zr_{0.95}Ce_{0.05}NiSn$ at weak magnetic fields (50 and 100 Oe) as a function of temperature.

instability by the destructive influence of alloying, and then several reasons for the gap formation are presented in the conclusions.

II. EXPERIMENT

The samples $Zr_{1-x}Ce_xNiSn$ and $Ti_{1-x}Ce_xNiSn$ were arc melted on a cooled copper crucible in a high-purity argon atmosphere and remelted ten times, and then annealed at 800 °C for one week. The constituents were specpure.

The x-ray analysis showed single-phase samples within the usual resolution of 6%. For Zr-Ni-Sn and the Ce alloys with $x=0.05$, 0.1 and 0.2, we found a cubic Mg-Ag-As structure,[15] which we also found in Ti-Ni-Sn and its Ce alloy with $x=0.05$. The solubility of Ce impurities in both matrices Zr-Ni-Sn and Ti-Ni-Sn is quite low. For larger values of x than $x=0.2$ and 0.05, respectively, in the x-ray-diffraction pattern we observed additional phases which were identified properely as $ZrNi_2Sn$ and $TiNi_2Sn$.

As we will show later, susceptibility measurements can detect phase segregation on a much finer scale than the x-ray analysis. A superconducting quantum interference device magnetometer and vibrating magnetometer were used to obtain magnetization results for low temperatures from 1.6 up to 300 K, and magnetic fields of 50–50 kOe.

The x-ray-photoemission spectra were obtained with monochromatized Al $K\alpha$ radiation at room temperature using a PHI 5600ci spectrometer. The spectra were measured immediately after cleaving the sample in vacuum below 6×10^{-10} Torr. Calibration of the spectra was performed according to Ref. 16. Binding energies were referenced to the Fermi level ($\epsilon_F=0$), the $4f$ levels of gold were found at 84.0 eV, and the observed energy spread of electrons detected at the Fermi energy was about 0.4 eV. In all investigated Ce alloys, in the x-ray photoemission spectra we detected a small amount of oxygen, which mainly arises from the impurity phase Ce_2O_3. This phase has also been detected in several single crystals of CeNiSn by other authors.[17]

The electronic structures of ordered Zr-Ni-Sn and Ti-Ni-Sn and the alloys were studied by the self-consistent tight-binding linearized muffin-Tin orbital (TB-LMTO) method[18] within the atomic-sphere approximation and the local-spin-density approximation. The exchange-correlation potential was assumed in the form proposed by von Barth-Hedin[19] and Langreth-Mehl-Hu,[20] (LMH) with corrections included. In the band calculations, we assumed the initial configurations according to the Periodic Table of elements. For Zr-Ni-Sn and Ti-Ni-Sn, for the calculations we considered a $C1_b$-type structure which consists of four interpenetrating fcc sublattices based on (0,0,0), $(\frac{1}{2}\ \frac{1}{2}\ \frac{1}{2})$, $(\frac{1}{4}\ \frac{1}{4}\ \frac{1}{4})$, and $(\frac{3}{4}\ \frac{3}{4}\ \frac{3}{4})$. In a $C1_b$-type structure, one of the sublattices, $(\frac{1}{4}\ \frac{1}{4}\ \frac{1}{4})$ or $(\frac{3}{4}\ \frac{3}{4}\ \frac{3}{4})$, is empty. The self-consistent band structures for $M_{1-x}Ce_xNiSn$ ($M=$Zr or Ti) alloys were calculated for the supercell structural model, which was built with two $C1_b$ cells along the z axis. In the supercell each fcc sublattice was divided into four simple cubic ones, and therefore our structural model consisted of 32 simple cubic sublattices. Each type of atom, (Zr,Ti), Ni, and Sn, and empty sphere (vacance) occupied eight simple cubic sublattices. The band calculations were performed for 93 k points in the irreducible wedge of the Brillouin zone. The electronic structures were computed for the experimental lattice parameters. The value of the Wigner-Seitz radii in the atomic-sphere approximation were chosen to satisfy the conditions: $\Sigma_n(S_n/S)^3=N$, where $S=a(3/4\pi N)^{1/3}$. Here a denotes the lattice parameter, N is the number of atoms in the cell, and the summation was made for all atoms in the cell.

III. RESULTS AND DISCUSSION

A. Magnetic properties

We present the magnetic susceptibility as a function of temperature for $Zr_{1-x}Ce_xNiSn$ ($x=0$ to 0.2) and $Ti_{1-x}Ce_xNiSn$ ($x=0$, 0.5) alloys. The magnetic properties of CeNiSn were discussed, e.g., in Ref. 9. The susceptibility

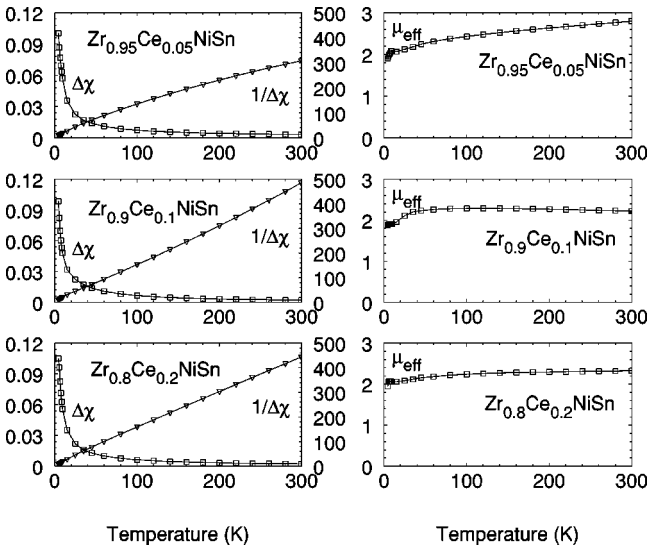

FIG. 3. Magnetic susceptibility $\Delta\chi$ in emu/(mole Ce) and inverse susceptibility $\Delta\chi^{-1}$ in $(\mathrm{cm}^3/\mathrm{mole\ Ce})^{-1}$. The applied magnetic field is 10 kOe. The plots on the right side present the effective magnetic moment μ_{eff} per one Ce atom in μ_B as a function of temperature [the effective magnetic moment at each T is $(\Delta\chi T)^{1/2}(3k_B/N)^{1/2}$, where k_B is the Boltzman constant and N the Avogadro number].

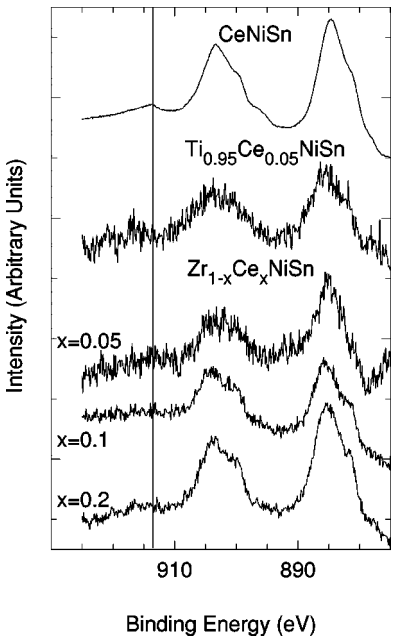

FIG. 4. Ce $3d$ XPS spectra obtained for several $M_{1-x}\mathrm{Ce}_x\mathrm{NiSn}$ alloys (M=Zr or Ti) are compared with the spectrum of Ce-Ni-Sn. The $3d^9 4f^1$ and $3d^9 4f^2$ components are separated on the basis of the Doniach-Šunjić theory. The line indicates the energy of the $3d^9 f^0$ satellite.

reminds one somehow of heavy-electron cerium-fluctuation compounds. At high temperatures it follows the Curie-Weiss law, with nearly the $J=\frac{5}{2}$ free-ion value of the effective moment (μ_{eff}), whereas at $T=0$ it reveals a singlet ground state. The ground state of the alloyd CeNiSn is still a singlet due to the Kondo coupling.[21,22] However, alloying destroys the semiconducting gap. At a very weak magnetic field the susceptibility either of CeNiSn or its alloys always indicates the presence of additional phases, mainly of Ce_2O_3, which contribute to a Brillouin term at low temperature. Even in very good quality single crystals,[17] the impurity phase was detected. Therefore, we have also analyzed Zr and Ti alloys at weak magnetic fields, at which the presence of additional Ce magnetic phases is less than 0.1%.

In this paper we attempt to answer experimentally the question of band-gap stability in the ternary intermetallic compounds Zr-Ni-Sn and Ti-Ni-Sn. At first, we present the magnetic susceptibility of these compounds, and then we show how it depends on alloying.

In Fig. 1 the susceptibilities of Zr-Ni-Sn and Ti-Ni-Sn are nearly temperature independent between 50 and 300 K, but below 50 K one observes an increase of the susceptibilities. We attribute this increase to metallurgical problems, which are also apparent in the strong resistivity dependence on the annealing, and correlate with the substitutional disorder between Zr or Ti and Sn atomic positions.[2]

At weak magnetic fields of 50 and 100 Oe, one observes a paramagnetic behavior for both samples, with a weak and constant magnetization above $T=3.7$ K. But below this temperature the magnetization becomes negative, which suggests an incomplete solution of Sn (less than 0.1%) which is superconducting with a characteristic temperature of $T_c=3.7$ K.

In Fig. 2 we show the magnetization of the 5% Ce alloy as a function of temperature and magnetic field. The magnetization increases below the temperature $T=5$ K and begins to saturate near 1.6 K. The incomplete solution effect of the matrix is covered by the ferromagnetic impurity Ce_2O_3 amount, discussed above. Figure 3 shows the susceptibility increment $\Delta\chi$ and $(\Delta\chi)^{-1}$ for $\mathrm{Zr}_{1-x}\mathrm{Ce}_x\mathrm{NiSn}$ alloys, where $\Delta\chi=(\chi(\mathrm{alloy})-\chi[(1-x)\mathrm{Zr\text{-}Ni\text{-}Sn}])/x$. At low temperatures one observes for the alloys only a weak concentration dependence of $\Delta\chi^{-1}$, which emphasizes the uncertainties of sample preparation. At high temperatures the concentration dependence becomes relatively stronger. We have also plotted $\Delta\chi T$ to exhibit this point more clearly. The kink of $\Delta\chi T$ near 5 K in all plots indicates the ferromagnetic clusters of Ce_2O_3. The Curie-Weiss Θ temperatures are negative. This suggests a spin-glass-type ordering, even for the 5% Ce sample. However, we did not observe a maximum of the susceptibility at the frozen temperature T_f. This type of behavior is, however, expected to be observed in the low-magnetic-field experiment below $T=1.6$ K.

The most important conclusion from Fig. 3 is the following. The high-temperature effective magnetic moment is close to the full $4f^1$ Hund's-rule ground-state moment of $2.54\mu_B$. Below 60 K a deviation from the high-temperature law occurs, giving, at 4.2 K, an effective moment of about $1.9\mu_B$. This behavior may be ascribed to crystal-field effect which has a ''preference'' for two low-lying doublets. The magnetic Ce ground state of the alloyed Zr or Ti Heusler alloys with the gap is in important contradiction with the nonmagnetic state of CeNiSn. The singlet ground state due to the Kondo coupling and the $4f$ Ce instability argue for the CeNiSn hybridization gap, which is destroyed when Ce or Ni are partly replaced by La or a d-type atom. In Ref. 21 we presented the Ce $3d$ XPS spectra, which did not show the shake-up satellite due to the $4f$ instability, when the CeNiSn sample is alloyed. The magnetic susceptibility

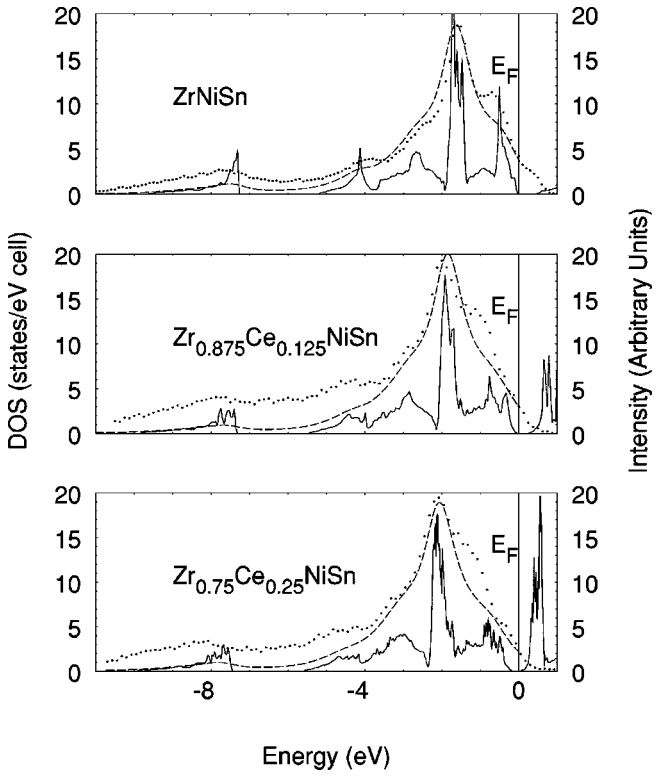

FIG. 5. Comparison of the total DOS (solid line), the convoluted DOS (by Lorentzians of the half-width 0.4 eV and taking into account proper cross sections for partial bands with different l-symmetry; dashed line), and the measured XPS valence bands corrected by the background (points) for $Zr_{1-x}Ce_xNiSn$.

clearly now indicates trivalent Ce in Zr-Ni-Sn or Ti-Ni-Sn materials. With alloying we expect to observe a drastic decrease of the gaps in the matrices bands, which should be proportional to the decrease of the number of tetravalent ions (Zr,Ti) in the unit cell.

B. Electronic properties of $M_{1-x}Ce_xNiSn$, $M=Zr,Ti$

As mentioned above, the susceptibility showed the magnetic ground state and the stable configuration of the $4f$ shell of Ce diluted in Zr and Ti matrices. Now we present the Ce $3d$ x-ray photoemission spectra which confirm it.

In the x-ray photoemission core spectra of Ce the $3d$ spin-orbit-split components (Fig. 4) do not show any additional structure at the higher-energy side in respect to the main $3d_{5/2}$ and $3d_{3/2}$ peaks, as a contribution of the $4f^0$ configuration to the Ce ground state.[23] This $3d^94f^0$ components for $3d$ multiplets are clear evidence of the mixed valence in Ce compounds; they are, however, not present in the $3d$ x-ray photoemission spectra of γ-Ce.[24] At the low-binding-energy side of the $3d_{5/2}$ and $3d_{3/2}$ lines (Fig. 4), shake-down satellites are observed, which are known to account for the screened Ce $3d^94f^2$ final state.[25–27] The structure in the Ce $3d$ x-ray photoemission spectra is interpreted in terms of the Gunnarsson-Schönhammer theory.[23] It is possible to determine the coupling Δ energy from the ratio $r=I(f^2)/[I(f^1)+I(f^2)]$ calculated in Ref. 28 as a function of Δ. Δ is defined as $\pi V^2\rho_{\max}$, where $\rho_{\max}$ is the maximum in density of conduction states and V is the hybridization matrix element. The separation of the peaks in the Ce $3d$

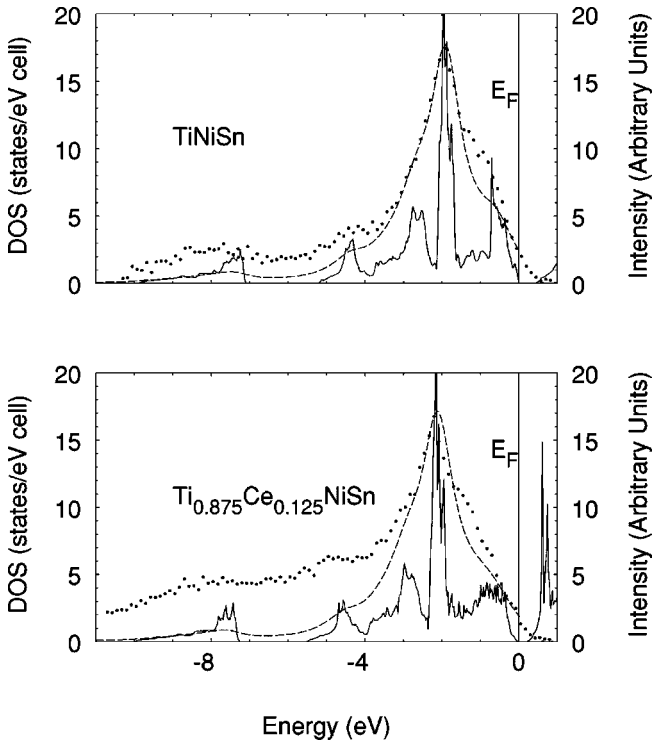

FIG. 6. The total DOS (solid line), the convoluted DOS as in Fig. 5 (dashed line), and the valence-band spectra (points).

XPS spectra (Fig. 4), which overlap, was made on the base of the Doniach-Šunjić theory.[29] In all Ce cases, only the $3d_{3/2}f^2$ peak intensities can be accurately estimated in relation to $3d^9f^1$, the $3d_{5/2}f^1$ peak overlaps the Sn $3s$ signal. In the peak fitting procedure we considered an additional contribution to the total intensity to find the theoretically intensity ratio 6:4 of the $3d_{5/2}$ and $3d_{3/2}$ peaks. The Sn $3s$ peak at 884 eV provides about 15% of the total intensity in 20% Ce alloy due to the $3d^94f^1$ final states. But its contribution de-

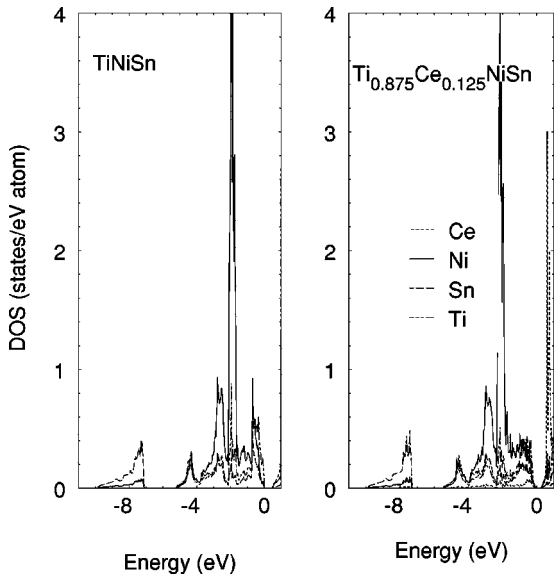

FIG. 7. The partial DOS for Ti-Ni-Sn and $Ti_{0.875}Ce_{0.125}NiSn$. Strongly hybridized states are visible in both compounds near the Fermi energy. Our calculations show almost the same plots for Zr-Ni-Sn and its Ce alloys.

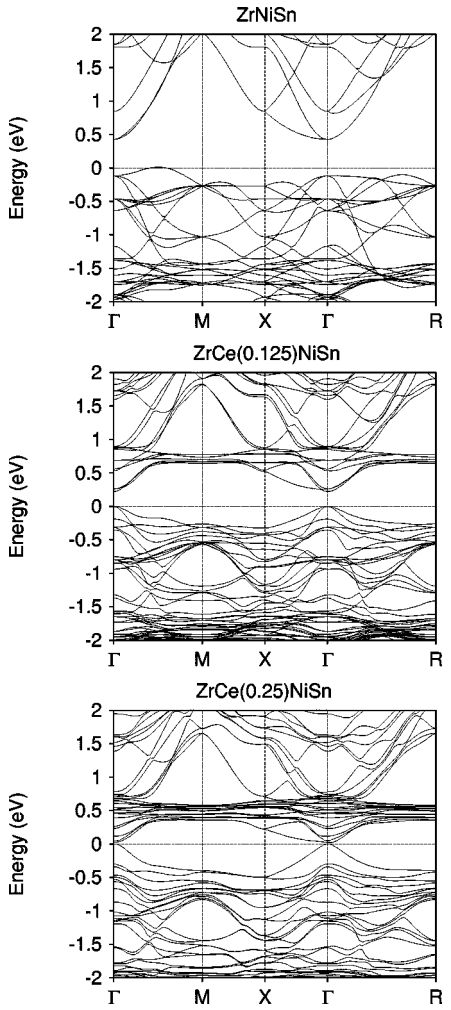

FIG. 8. TB LMTO band structure of $Zr_{1-x}Ce_xNiSn$ along various symmetry directions in the Brillouin zone.

pends on the Ce concentration and increases when the Ce content in the alloy decreases. The intensity ratio is $r \approx 0.20$ for 20% Ce alloy and slightly increases with decreasing of x. From the calculated variation of r as a function of Δ in Ref. 28, this value gives a hybridization width of about 100 meV for $Zr_{0.8}Ce_{0.2}NiSn$ which increases with dilution. The dependence of r on other parameters, such as the f-level occupancy, and U, the Coulomb interaction between f electrons, is weaker,[28] and we neglect this dependence in our calculations. For the Ce 5% sample, Δ is about 150 meV. With an increasing dilution of Ce, the Ce average distance increases, thus the increase of Δ with increasing Zr concentration arises from an overlap with d orbitals on the neighboring atoms. This analysis suggests the visible hybridization effect in the valence bands. Figures 5 and 6 compare the x-ray photoemission (XPS) valence bands of $Zr_{1-x}Ce_xNiSn$ and $Ti_{1-x}Ce_xNiSn$ alloys with the calculated total densities of states (DOS's). The DOS's are convoluted by a Lorentzian of half-width equal to 0.4 eV, and evaluated by a proper cross sections for partial states on each atom of the unit cell, which are taken from Ref. 30. All XPS bands are subtracted by the backgrounds which have been calculated with the well validated and described Tougaard algorithms.[31] The agreements between the experimental and calculated spectra are good. The sharp peaks located at 2 eV in the bands are

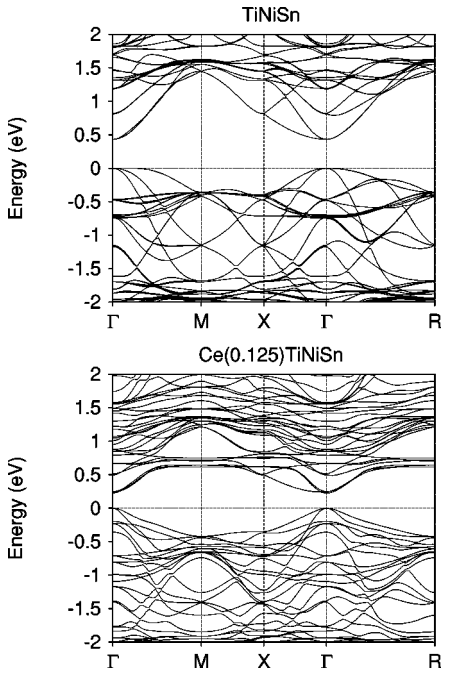

FIG. 9. TB LMTO band structure of $Ti_{1-x}Ce_xNiSn$ along various symmetry directions in the Brillouin zone.

mainly attributed to $3d$ Ni states. The second peak 0.5 eV below the Fermi level in the MNiSn DOS represents the strongly hybridized Ni-Zr or Ni-Ti d states. Its intensity decreases rapidly when the M element is in 10% replaces by Ce. Figures 5, 6, and 7 show the Ce f states located at 0.7 eV (10% Ce sample) or at 0.5 eV (20% Ce sample) above the Fermi level, but in both cases the tail of the f states strongly hybridizes with Ni and Zr or Ti d states. This hybridization makes a reduction of the DOS intensities of d states near ϵ_F, and destroys the gap. The destructive influence on the gap formation can also be visible in Figs. 8, and 9, which show the bands plotted along various symmetry directions. At the Γ point the gap, opened for MNiSn, is now closed or strongly reduced when Ce replaces the M metal. For both Zr-Ni-Sn and Ti-Ni-Sn alloys, the indirect gap at the Γ point has the same value and does not depend on the atomic number Z of the M element. We found a large rate of depression for this gap due to Ce impurities, which again does not depend on the Z number, and is about 1.6 eV/(Ce atom). The zero-gap limit in the alloys is reached at a critical concentration of Ce impurities close to the limit of Ce dilution without segregation of additional phases. This also means that the hybridization gap characterizes the MNiSn-type alloys (M = Zr,Ti,Hf) and has an important influence on their structural properties.

The broad peaks detected at 8 eV in the XPS valence bands (Figs. 5 and 6) are connected with Sn s electronic states. There is a second gap in the bands between 5 and 7 eV, which is characteristic of semi-Heusler alloys and Ce-Ni-Sn-type intermetallics.

IV. CONCLUSIONS

MNiSn semi-Heusler alloys, where M is tetravalent Zr or Ti, are strongly hybridized materials with a gap of the order at 500 meV. This gap is formed for a tetravalent element M,

which strongly hybridizes with the conduction-band states. When M is partly replaced by a trivalent Ce, the gap is depressed, and it vanishes almost at the same concentration of about 25% of Ce impurities. Ce atoms diluted in MNiSn matrices are detected as trivalent impurities with a magnetic ground state. The Ce f states are strongly hybridized with M and Ni d states near the Fermi level. The hybridization energy Δ was determined from the Ce $3d$ XPS spectra for each Ce alloy on the base of Gunnarsson and Schönhammer theory. Δ is about 100–150 meV, depending on the Ce content in Zr-Ni-Sn or Ti-Ni-Sn. A strong f-d hybridization shifts the unoccupied states to the Fermi level, and as a consequence destroys the gap. Similar band properties are known in CeNiSn semiconductors with metallic elements. In this case Ce is in a mixed-valence state, and in contrast to the diluted Ce alloys it has a nonmagnetic ground state of the Kondo-type. We classified the cubic semi-Heusler MNiSn and the orthorombic CeNiSn compounds to a group of alloys with a hybridization gap at the Fermi energy. The tetravalent M element in MNiSn-type semiconducting alloys seems for us to be very important. The gap is suppressed by a partial substitution of a trivalent metal (e.g., Ce) either for Zr^{4+} or Ti^{4+}. In consequence, this substitution gives an average value of the valence v at the M-atom position in $M_{1-x}Ce_x$NiSn systems less than 4, and $v=3+\nu$, where $\nu=1-x$. The $Zr_{1-x}Ce_x$NiSn system shows a linear scaling of the gap ΔE with ν. Considering the influence of the valence of the M element on the gap formation, a very crude analysis predicts a gap $\Delta E\nu$ of about 20 meV for CeNiSn with a slightly mixed valence of Ce ions, if one takes into consideration $\Delta E(\text{Zr-Ni-Sn}, \nu=1)=430$ meV. This value is, however, 20 times larger than what was measured, but shows the strong influence of the valence of the M atom on the gap formation in MNiSn-type intermetallics. We have mentioned the rapid change of Ni d DOS closed to ϵ_F when MNiSn is alloyed. Recently we have theorized that a very similar effect, observed in CeNiSn when Ni is partly substituted with Cu or Pd, is due to the charge transfer.

ACKNOWLEDGMENTS

This work was partly supported by the Foundation for Polish Science Project: SUBIN No. 10/95), by the Deutscher Akademischer Austausch Dienst (DAAD), and by the Deutsche Forschungsgemeinschaft (DFG). One of us (A.J.) thanks the State Committee for Scientific Research for financial support (Project No. 2P30200507). The calculations were made in the Supercomputing and Networking Center of Poznań.

[1] F. G. Aliev *et al.*, Fiz. Nizk. Temp. **13**, 498 (1987) [Sov. J. Low Temp. Phys. **13**, 281 (1987)]; F. G. Aliev *et al.*, Pis'ma Zh. Eksp. Teor. Fiz. **45**, 535 (1987) [JETP Lett. **45**, 684 (1987)].
[2] F. G. Aliev *et al.*, Z. Phys. B **75**, 167 (1989).
[3] F. G. Aliev *et al.*, Z. Phys. B **80**, 353 (1990).
[4] S. Öğüt and K. M. Rabe, Phys. Rev. B **51**, 10 443 (1995).
[5] A. Ślebarski, A. Jezierski, M. Neumann, and S. Plogmann (unpublished).
[6] R. A. de Groot, F. M. Mueller, P. G. van Engen, and K. H. J. Buschow, Phys. Rev. Lett. **50**, 2024 (1983).
[7] J. Tobola *et al.*, J. Magn. Magn. Mater. **159**, 192 (1996).
[8] T. Takabatake *et al.*, Jpn. J. Appl. Phys., Suppl. **26**, 547 (1987).
[9] T. Takabatake *et al.*, Phys. Rev. B **41**, 9607 (1990).
[10] S. K. Malik and D. T. Adroja, Phys. Rev. B **43**, 6277 (1991).
[11] M. F. Hundley *et al.*, Phys. Rev. B **42**, 6842 (1990).
[12] T. Takabatake *et al.*, J. Magn. Magn. Mater. **76/77**, 87 (1988).
[13] A. Ślebarski and D. Wohlleben, Z. Phys. B **60**, 449 (1985).
[14] A. Ślebarski, D. Wohlleben, and P. Weidner, Z. Phys. B **61**, 177 (1985).
[15] W. Jeitschko, Metall. Tran. **1**, 3159 (1970).
[16] Y. Baer, G. Busch, and P. Cohn, Rev. Sci. Instrum. **46**, 466 (1975).
[17] G. Nakamoto *et al.*, J. Phys. Soc. Jpn. **64**, 4834 (1995).
[18] O. K. Andersen, O. Jepsen, and M. Sob, in *Electronic Structure and Its Applications*, edited by M. Yussouff (Springer, Berlin, 1987), p. 2.
[19] U. von Barth and L. Hedin, J. Phys. C **5**, 1629 (1972).
[20] C. D. Hu and D. C. Langreth, Phys. Scr. **32**, 391 (1985).
[21] A. Ślebarski *et al.*, Phys. Rev. B **54**, 13 551 (1996).
[22] A. Ślebarski *et al.*, Phys. Rev. B **56**, 7245 (1997).
[23] O. Gunnarsson and K. Schönhammer, Phys. Rev. B **28**, 4315 (1983).
[24] E. Wuilloud, H. R. Moser, W. Schneider, and Y. Baer, Phys. Rev. B **28**, 7354 (1984).
[25] G. K. Wertheim, R. L. Cohen, A. Rosencweig, and H. J. Guggenheim, in *Electron Spectroscopy*, edited by D. A. Shirley (North-Holland, Amsterdam, 1972), p. 813.
[26] G. Crecelius, G. K. Wertheim, and D. N. E. Buchanan, Phys. Rev. B **18**, 6519 (1978).
[27] J. C. Fuggle *et al.*, Phys. Rev. Lett. **45**, 1597 (1980).
[28] J. C. Fuggle *et al.*, Phys. Rev. B **27**, 7330 (1983).
[29] S. Doniach and M. Šunjić, J. Phys. C **3**, 285 (1970).
[30] J. J. Yeh and I. Lindau, At. Data Nucl. Data Tables **32**, 1 (1985).
[31] S. Tougaard and P. Sigmund, Phys. Rev. B **25**, 4452 (1982).